

Studying bona fide SARS-CoV-2 biology in a BSL-2 biosafety environment using a split-virus-genome system

Yingxin Ma^{1†*}, Guobin Mao^{1†}, Weishan Yang^{1,2†}, Guoqiang Wu¹, Guoqiang Li¹, Xiaoying Li¹, Xin Lin¹, Junnan Lu¹, Shijun Zhao^{1,2}, Wei Zhao¹, Junbiao Dai^{1*} & Xian-En Zhang^{3,4*}

¹CAS Key Laboratory of Quantitative Engineering Biology, Guangdong Provincial Key Laboratory of Synthetic Genomics and Shenzhen Key Laboratory of Synthetic Genomics, Shenzhen Institute of Synthetic Biology, Shenzhen Institute of Advanced Technology, Chinese Academy of Sciences, Shenzhen 518055, China;

²University of Chinese Academy of Sciences, Beijing 100049, China;

³Faculty of Synthetic Biology, Shenzhen Institute of Advanced Technology, Chinese Academy of Sciences, Shenzhen 518055, China;

⁴National Key Laboratory of Biomacromolecules, CAS Center for Biological Macromolecules, Institute of Biophysics, Chinese Academy of Sciences, Beijing 100101, China

Received March 17, 2022; accepted April 22, 2022; published online May 12, 2022

Citation: Ma, Y., Mao, G., Yang, W., Wu, G., Li, G., Li, X., Lin, X., Lu, J., Zhao, S., Zhao, W., Dai, J., and Zhang, X.E. (2022). Studying bona fide SARS-CoV-2 biology in a BSL-2 biosafety environment using a split-virus-genome system. *Sci China Life Sci* 65, 1894–1897. <https://doi.org/10.1007/s11427-022-2114-8>

Dear Editor,

Severe acute respiratory syndrome coronavirus 2 (SARS-CoV-2) was identified as the pathogen causing the coronavirus disease (COVID-19), which sometimes resulted in fatal pneumonia (Hu et al., 2021). SARS-CoV-2 is a biosafety level 3 (BSL-3) pathogen, and the requirement for high containment conditions is a bottleneck for basic research on viral biology. To help general researchers who wish to study SARS-CoV-2 but do not have access to a BSL-3 facility, a system that (1) can mimic the real life cycle of the virus; (2) allows easy genetic manipulation; and (3) shows high biosafety in BSL-2 laboratory is required. Figure 1A depicts the split-virus-genome (SVG) system in which the full-length SARS-CoV-2 cDNA was divided into three parts, including SARS-CoV-2 S, ORF1ab, and StruΔS fragments (Jiang et al., 2021). The corresponding plasmids were co-transfected into 293T cells to form infectious virus, named “reconstituted SARS-CoV-2” (rSARS-CoV-2). Due to the

presence of packaging signal (PS) sequence, only one RNA (the one encoding ORF1ab) can be incorporated in rSARS-CoV-2 (Hsieh et al., 2005). Since rSARS-CoV-2 lacked all structural genes, no progeny virus was produced. Therefore, rSARS-CoV-2 can serve as a safe and universal platform for virological research.

To ensure the expression of each component, we co-transfected cells with one, two, or three plasmids. As shown in Figure S1C in Supporting Information, transfection of S plasmid resulted in the production of S protein. StruΔS-EGFP plasmid was transfected to study the activity of StruΔS (Figure S1A–S1C in Supporting Information). Transmission electron microscopy (TEM) imaging showed that the expressed structural proteins were assembled into reconstituted virus particles (rVPs) without spike proteins (Figure 1B). N protein was verified to be packaged into rVPs (StruΔS) (Figure S1D in Supporting Information). ORF1ab-mCherry construct was used to verify ORF1ab expression (Figure S1A and S1C in Supporting Information). Next, we attempted to co-express two plasmids, and successfully obtained rVPs (StruΔS-S) and rVPs (StruΔS-ORF1ab) (Figure 1B and Figure S1D in Supporting Information).

†Contributed equally to this work

*Corresponding authors (Xian-En Zhang, email: zhangxe@ibp.ac.cn; Junbiao Dai, email: junbiao.dai@siat.ac.cn; Yingxin Ma, email: mayingxin23@163.com)

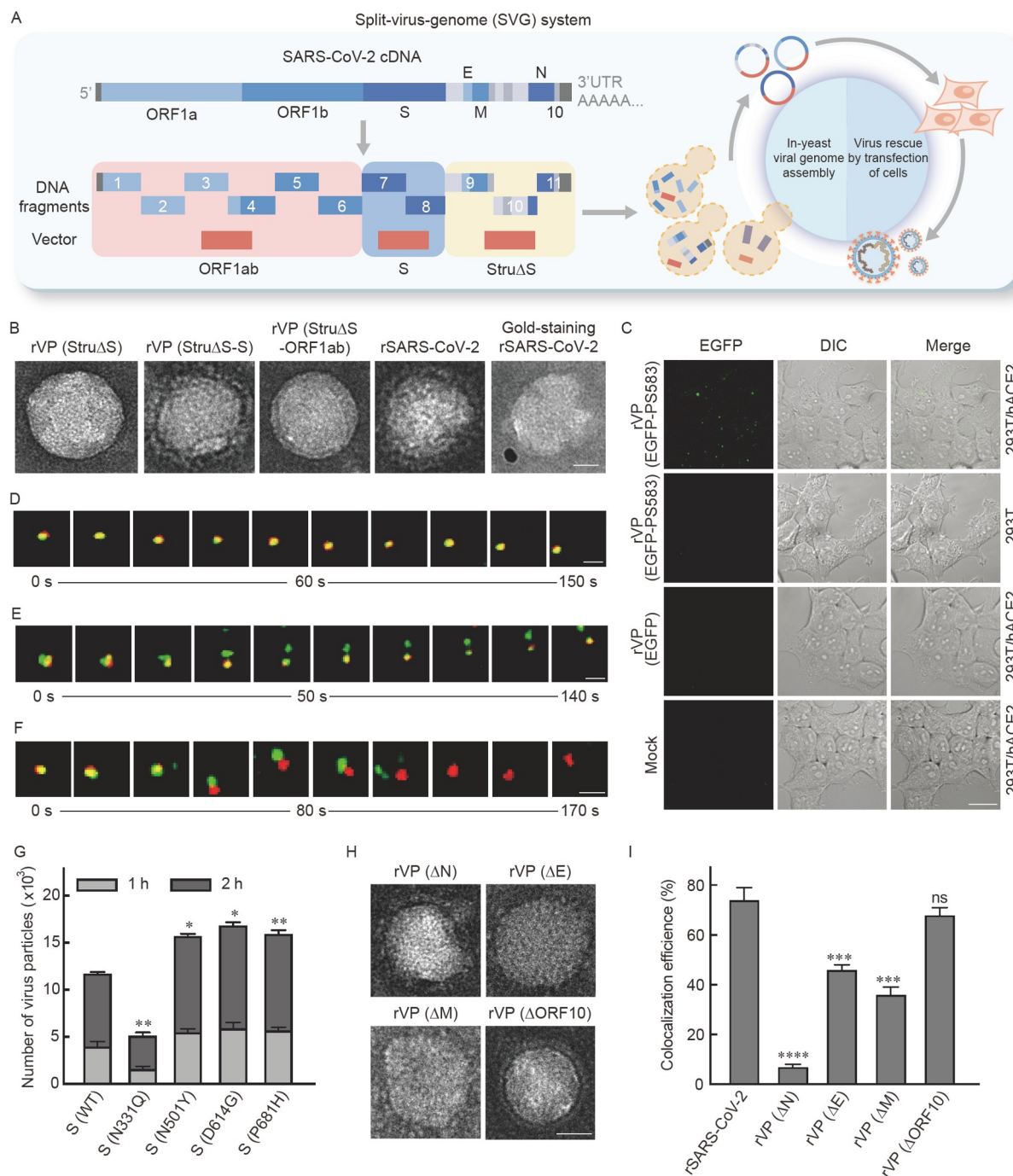


Figure 1 Design, construction, and applications of the SVG system. **A**, Schematic of the full-length SARS-CoV-2 genome and the split sections. The DNA fragments were assembled in yeast to construct SARS-CoV-2 S, ORF1ab, and StruΔS plasmids. **B**, Morphology of rSARS-CoV-2 and rVPs. rSARS-CoV-2 also visualized using immuno-gold staining with spike protein antibody. Scale bar: 20 nm. **C**, Confocal microscopy images of EGFP fluorescence in rVPs (EGFP-PS583)-infected 293T/hACE2 cells, rVPs (EGFP-PS583)-infected 293T cells, and rVPs (EGFP)-infected 293T/hACE2 cells at 48 h post infection. Scale bar: 20 μm. **D-E**, Sequential snapshots of (D) rSARS-CoV-2 (QD-DiO) entry into a 293T/hACE2 cell, (E) the dissociation of RNA-QD and Env-DiO in a 293T/hACE2 cell, (F) rSARS-CoV-2 (QD-DiO) entry into a 293T/hACE2-hTMPRSS2 cell. Scale bar: 2 μm. **G**, Statistical analysis of the number of DiO-labeled rSARS-CoV-2 and rVPs (mut) in cytoplasm. **H**, Morphology of mutated rVPs. Scale bar: 20 nm. **I**, Co-localization of DiO and QD signals in rSARS-CoV-2 (QD-DiO) and mutated rVPs (QD-DiO).

Three plasmids were co-transfected to generate rSARS-CoV-2 (Figure S2A-S2B in Supporting Information). TEM showed round particles with typical crown of spikes, which was confirmed by immune-gold labeling (Figure 1B). S and

N proteins assembled into virions were analyzed using western blot (Figure S2B in Supporting Information). Viral infectivity was quantified by tissue culture infectious dose (TCID₅₀)/mL titer, with lg TCID₅₀/mL=1.5. To address po-

tential biosafety concerns, the rescued virus was first tested in BSL-3 laboratory. 293T/hACE2 cells were constructed and infected with rSARS-CoV-2 (Figure S3A in Supporting Information). Viral structural proteins were not detected in cell lysate and supernatant collected from infected cells (Figure S3B in Supporting Information). Representative images of 293T/hACE2 cells infected with rSARS-CoV-2 and wild-type SARS-CoV-2 revealed significant differences in viral titers, which was due to the inability of rSARS-CoV-2 to replicate (Kim et al., 2020) (Figure S3C in Supporting Information). Therefore, rSARS-CoV-2 was confirmed to be a safe model for the study of virus biology. The assembly of viral genomic RNA in virions was examined by infecting 293T/hACE2 cells with rSARS-CoV-2 (Figure S2C in Supporting Information). The mCherry signal was observed in infected cells, but it was very weak, owing to the inability of ORF1ab to replicate (Figure S2D–S2E in Supporting Information). Fluorescence was not detectable in rVPs (mCherry)-infected cells, suggesting that mCherry mRNA failed to be packaged into particles. SARS-CoV-2 PS located in ORF1ab was thus necessary for the assembly of viral RNA into particles.

Viral genome incorporation is mediated by the interaction between nucleocapsid protein and PS sequence. We predicted the location of SARS-CoV-2 PS near the 3' terminus of ORF1b using previously characterized SARS-CoV PS (Kim et al., 2020). There were two stable stem-loops (SL1 and SL2) in the predicted RNA secondary structures of these regions in SARS-CoV-2, SARS-CoV, and bat SARS-like CoV (Figure S4A in Supporting Information). Multiple alignment confirmed the high conservation of RNA stem-loops, which may act as PS in SARS-CoV-2 (Figure S4B in Supporting Information). To test this hypothesis and experimentally examine packaging activity, we selected two regions containing the conserved stem-loop structure, PS101 (nt 19900–20000) and PS583 (nt 19773–20335). The plasmids pEGFP-N1-PS101 and pEGFP-N1-PS583 were constructed and co-transfected into 293T cells with S and Stru Δ S constructs, respectively. The transcription and expression of EGFP-PS101 and EGFP-PS583 RNA were first verified (Figure S5A–S5C in Supporting Information). Next, rVPs were isolated and their integrity was monitored (Figure S5D in Supporting Information). The GFP signal was observed within rVPs (EGFP-PS101)- or rVPs (EGFP-PS583)-infected cells (Figure 1C and Figure S5E–S5F in Supporting Information). The higher fluorescence intensity of PS583 implied that EGFP-PS583 RNA had better packaging activity. rVPs (EGFP)-infected cells failed to show GFP fluorescence, indicating that in the absence of PS sequence, EGFP mRNA itself cannot be packaged into rVPs (EGFP). These results suggested that putative PS sequence lied in the 101 bp sequence near the 3' end of ORF1b, and was vital for the assembly of viral genomic RNA.

The SVG system was attempted to visualize the process of rSARS-CoV-2 infection in real time. Dual-fluorescent virions, rSARS-CoV-2 (QD-DiO), was first generated by labeling viral RNA with quantum dot (QD) nanobeacon and labeling viral envelop with DiO (Ma et al., 2021) (Figure S6A–S6C in Supporting Information). To study the dynamic process of viral entry, rSARS-CoV-2 (QD-DiO) was incubated with 293T/hACE2 cells. A dual-color particle was initially observed on cell membrane, and then transported into host cell in an active manner (Figure 1D, Figure S6D–6F and Video S1 in Supporting Information). The release of viral core from the envelope during endocytic entry into host cells was also captured. A separation of the red dot from the green dot was observed during the dynamic movement of the virion (Figure 1E, Figure S6G–S6I and Video S2 in Supporting Information). The escape of viral core from endosome was necessary for successful infection. rSARS-CoV-2 (QD-DiO) was also used to infect 293T/hACE2-hTMPRSS2 cells. Lipid DiO fluorescence disappeared at cell surface and the QD-labeled viral core separated rapidly from cell membrane, suggesting virus entry via plasma membrane fusion in the presence of TMPRSS2 (Hoffmann et al., 2020) (Figure 1F and Video S3 in Supporting Information).

Theoretically, the SVG system can quickly generate and test mutations throughout the viral genome. Four mutations were induced at different regions in S protein (Figure S7A in Supporting Information). The mutated S protein was assembled into rVPs (mut), which were similar in morphology and size to rSARS-CoV-2 (Figure S7B in Supporting Information). rVPs (N501Y), rVPs (D614G), and rVPs (P681H) showed higher infectivity than rSARS-CoV-2, but the infectivity of rVPs (N331Q) was significantly lower (Figure 1G), consistent with previous reports (Li et al., 2020). The SVG system was further used to systematically investigate the requirements of structural proteins in viral assembly and RNA packaging. Since ORF10 is a newly acquired ORF that is specific to SARS-CoV-2, we also included it in our study (Pancer et al., 2020). Using Stru Δ S-EGFP as a template, four plasmids with deletion of N, E, M, or ORF10 gene were constructed (Bai et al., 2022) (Figure S8A in Supporting Information). TEM imaging showed that spherical rVPs with coronal structures can still be produced by deleting N, E, M, or ORF10 (Figure 1H). N and S proteins were present in all these rVPs, except for rVPs (Δ N), in which N protein was absent (Figure S8B in Supporting Information). This indicated that none of these genes was necessary for rVPs assembly. To test viral RNA packaging, we examined ORF1ab-mCherry signal in rVPs-infected cells. rVPs (Δ ORF10)-infected cells showed red fluorescence, while rVPs (Δ N), rVPs (Δ E), and rVPs (Δ M) failed to produce any fluorescence signal (Figure S8C in Supporting Information). Then, we further verified the incompleteness of viral packaging through the above dual-labeling. The co-

localization efficiency of rVPs (Δ ORF10) was similar to that of rSARS-CoV-2 (~70%), whereas that of rVPs (Δ E) and rVPs (Δ M) were significantly lower. A sharp reduction in co-localization efficiency was observed when N protein was absent (Figure 1I and Figure S8D in Supporting Information). These results suggested that N is essential for viral RNA packaging and ORF10 is unnecessary, whereas E and M are important but not necessary.

In summary, we designed a novel and universal platform called the SVG system to advance research on each functional component of large-size viruses. Here, the full-length SARS-CoV-2 cDNA was split into three fragments, and co-transfected into cells to produce single-round infectious rSARS-CoV-2. Using rSARS-CoV-2, we systematically analyzed the function of multiple components and visualized viral life cycle in real time. The SVG system can serve as a powerful tool to dissect authentic viology in BSL-2 laboratory and facilitate methods development to cease the epidemic.

Compliance and ethics The author(s) declare that they have no conflict of interest. J.D., Y.M., and G.M. have filed a patent on the split-viral-genome system of SARS-CoV-2. The SARS-CoV-2 genomes used in this study are according with Genbank #MN908947-3. The materials used in this study are listed in Supplementary Materials.

Acknowledgements We are grateful to Dr. Xiaoping Xiao at Shenzhen Center for Disease Control and Prevention for help on the biosafety test in BSL-3 laboratory. This work was supported by Strategic Priority Research Program of the Chinese Academy of Sciences, China (XDB29050100), National Natural Science Foundation (21890743, 31725002), Youth Innovation Promotion Association CAS (2021359), Natural Science Foun-

dation of Guangdong (2018B030306046, 2020A1515111130), Shenzhen Science and Technology Program (KQTD20180413181837372), Guangdong Provincial Key Laboratory of Synthetic Genomics (2019B030301006) and Shenzhen Outstanding Talents Training Fund.

References

- Bai, C., Zhong, Q., and Gao, G.F. (2022). Overview of SARS-CoV-2 genome-encoded proteins. *Sci China Life Sci* 65, 280–294.
- Hoffmann, M., Kleine-Weber, H., Schroeder, S., Krüger, N., Herrler, T., Erichsen, S., Schiergens, T.S., Herrler, G., Wu, N.H., Nitsche, A., et al. (2020). SARS-CoV-2 cell entry depends on ACE2 and TMPRSS2 and is blocked by a clinically proven protease inhibitor. *Cell* 181, 271–280.e8.
- Hsieh, P.K., Chang, S.C., Huang, C.C., Lee, T.T., Hsiao, C.W., Kou, Y.H., Chen, I.Y., Chang, C.K., Huang, T.H., and Chang, M.F. (2005). Assembly of severe acute respiratory syndrome coronavirus RNA packaging signal into virus-like particles is nucleocapsid dependent. *J Virol* 79, 13848–13855.
- Hu, B., Guo, H., Zhou, P., and Shi, Z.L. (2021). Characteristics of SARS-CoV-2 and COVID-19. *Nat Rev Microbiol* 19, 141–154.
- Jiang, S., Tang, Y., Xiang, L., Zhu, X., Cai, Z., Li, L., Chen, Y., Chen, P., Feng, Y., Lin, X., et al. (2021). Efficient de novo assembly and modification of large DNA fragments. *Sci China Life Sci*, doi: 10.1007/s11427-021-2029-0.
- Kim, D., Lee, J.Y., Yang, J.S., Kim, J.W., Kim, V.N., and Chang, H. (2020). The architecture of SARS-CoV-2 transcriptome. *Cell* 181, 914–921.e10.
- Li, Q., Wu, J., Nie, J., Zhang, L., Hao, H., Liu, S., Zhao, C., Zhang, Q., Liu, H., Nie, L., et al. (2020). The impact of mutations in SARS-CoV-2 spike on viral infectivity and antigenicity. *Cell* 182, 1284–1294.e9.
- Ma, Y., Mao, G., Wu, G., Chen, M., Qin, F., Zheng, L., and Zhang, X.E. (2021). Dual-fluorescence labeling pseudovirus for real-time imaging of single SARS-CoV-2 entry in respiratory epithelial cells. *ACS Appl Mater Interfaces* 13, 24477–24486.
- Pancer, K., Milewska, A., Owczarek, K., Dabrowska, A., Kowalski, M., Labaj, P.P., Branicki, W., Sanak, M., and Pyrc, K. (2020). The SARS-CoV-2 ORF10 is not essential *in vitro* or *in vivo* in humans. *PLoS Pathog* 16, e1008959.

SUPPORTING INFORMATION

The supporting information is available online at <https://doi.org/10.1007/s11427-022-2114-8>. The supporting materials are published as submitted, without typesetting or editing. The responsibility for scientific accuracy and content remains entirely with the authors.